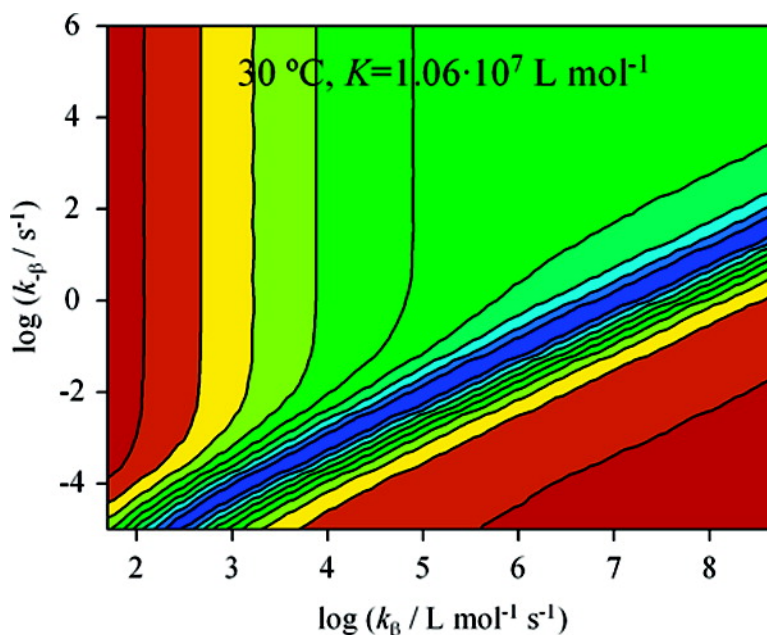Article

Consistent Experimental and Theoretical Evidence for Long-Lived Intermediate Radicals in Living Free Radical Polymerization

Achim Feldermann, Michelle L. Coote, Martina H. Stenzel, Thomas P. Davis, and Christopher Barner-Kowollik

More About This Article

Additional resources and features associated with this article are available within the HTML version:

- Supporting Information
- Links to the 12 articles that cite this article, as of the time of this article download
- Access to high resolution figures
- Links to articles and content related to this article
- Copyright permission to reproduce figures and/or text from this article

View the Full Text HTML

Consistent Experimental and Theoretical Evidence for Long-Lived Intermediate Radicals in Living Free Radical Polymerization

Achim Feldermann,[†] Michelle L. Coote,*,[‡] Martina H. Stenzel,[†]
Thomas P. Davis,[†] and Christopher Barner-Kowollik*,[†]

*Contribution from the Centre for Advanced Macromolecular Design, School of
Chemical Engineering and Industrial Chemistry, The University of New South Wales,
Sydney, NSW 2052, Australia, and Research School of Chemistry, Australian National
University, Canberra, ACT 0200, Australia*

Received June 23, 2004; E-mail: mcoote@rsc.anu.edu.au; camd@unsw.edu.au

Abstract: The cumyl dithiobenzoate (CDB)-mediated reversible addition fragmentation chain transfer (RAFT) polymerization of styrene at 30 °C is studied via both kinetic experiments and high-level ab initio molecular orbital calculations. The kinetic data clearly indicate the delayed onset of steady-state behavior. Such an observation is consistent with the slow fragmentation model for the RAFT process, but cannot be reconciled with the cross-termination model. The comprehensive failure of the cross-termination model is quantitatively demonstrated in a detailed kinetic analysis, in which the independent influences of the pre-equilibria and main equilibria and the possible chain length dependence of cross-termination are fully taken into account. In contrast, the slow fragmentation model can describe the data, provided the main equilibrium has a large fragmentation constant of at least 8.9×10^6 L mol^{-1}. Such a high equilibrium constant (for both equilibria) is consistent with high-level ab initio quantum chemical calculations ($K = 7.3 \times 10^6$ L mol^{-1}) and thus appears to be physically realistic. Given that the addition rate coefficient for macroradicals to (polymeric) RAFT agent is 4×10^6 L mol^{-1} s^{-1}, this implies that the lifetime of the RAFT adduct radicals is close to 2.5 s. Since the radical is also kinetically stable to termination, it can thus function as a radical sink in its own right.

1. Introduction

Reversible addition fragmentation chain transfer (RAFT) polymerization[1–3] has—along with other equally important living free radical techniques[4,5]—revolutionized free radical polymerization, as it allows for the generation of complex macromolecular architectures such as comb, star, and block copolymers with narrow polydispersities. RAFT polymerization is increasingly finding applications for generating novel structures and materials in bioengineering and nanotechnology applications. Lowe et al. used copolymers made by RAFT to stabilize transition metal nanoparticles,[6] and materials based on nano- and

microporous polymers have also been reported.[7,8] Other applications include the manufacture of biocompatible nanocontainers for drug delivery applications.[9]

The RAFT approach was developed by the CSIRO group,[1] combining their earlier work on addition–fragmentation reactions of macromonomers[10] with the small radical chemistry of Zard and co-workers.[11] In a typical RAFT process, thiocarbonylthio compounds (known as RAFT agents, see Scheme 1) reversibly react with the growing polymeric radical via the chain transfer reaction depicted in Scheme 1. This reversible addition–fragmentation equilibrium is superimposed on a conventional free radical polymerization process. Ideally, the chain transfer process should be fast and the intermediate RAFT-adduct radical should be short-lived. Because of the rapid transfer of the growing polymeric radicals between their free and dormant forms, unwanted radical–radical termination processes are minimized without reducing the rate of propagation and hence polymerization. However, in several RAFT systems, a significant reduction of the rate of polymerization—compared with

[†] The University of New South Wales.

[‡] Australian National University.

(1) Mayadunne, R. T. A.; Rizzardo, E.; Chiefari, J.; Chong, Y. K.; Moad, G.; Thang, S. H. *Macromolecules* **1999**, *32*, 6977−6980. Chiefari, J.; Mayadunne, R. T. A.; Moad, C. L.; Moad, G.; Rizzardo, E.; Postma, A.; Skidmore, A.; Thang, S. H. *Macromolecules* **2003**, 36, 2273−2283. Moad, G.; Chiefari J, Mayadunne, R. T. A.; Moad, C. L.; Postma, A.; Rizzardo, E.; Thang, S. H. *Macromol. Symp.* **2002**, *182*, 65−80. Moad, G.; Chiefari, J.; Chong, Y. K.; Krstina, J.; Mayadunne R. T. A.; Postma, A.; Rizzardo, E.; Thang S. H. *Polym. Int.* **2000**, *49*, 993−1001.

(2) Donovan, M. S.; Lowe, A. B.; Sumerlin, B. S.; McCormick, C. L. *Macromolecules* **2002**, *35*, 4123−4123.

(3) Barner-Kowollik, C.; Davis, T. P.; Heuts, J. P. A.; Stenzel, M. H.; Vana, P.; Whittaker, M. *J. Polym. Sci. Polym. Chem.* **2003**, *41*, 365−375.

(4) Hawker, C. J.; Bosman, A. W.; Harth, E. *Chem. Rev.* **2001**, *101*, 3661−3688.

(5) Wang, J. S.; Matyjaszewski, K. *J. Am. Chem. Soc.* **1995**, *117*, 5614−5615. Haddleton, D. M.; Crossman, M. C.; Dana, B. H.; Duncalf, D. J.; Heming, A. M.; Kukulj, D.; Shooter, A. J. *Macromolecules* **1999**, *32*, 2110−2119.

(6) Lowe, A. B.; Sumerlin, B. S.; Donovan, M. S.; McCormick, C. L. *J. Am. Chem. Soc.* **2002**, *124*, 11562−11563.

(7) Barner-Kowollik, C.; Dalton, H.; Davis, T. P.; Stenzel, M. H. *Angew. Chem. Int. Ed.* **2003**, *42*, 3664−3668.

(8) Stenzel-Rosenbaum, M.; Davis, T. P.; Fane, A. G.; Chen, V. *Angew. Chem., Int. Ed.* **2001**, *40*, 3428−3432.

(9) Stenzel, M. H.; Barner-Kowollik, C.; Davis, T. P.; Dalton, H. *Macromol. Biosci.* **2004**, *4*, 445−453.

Scheme 1. Fundamental Reaction Sequence Describing the Reversible Chain Transfer Equilibrium Operative during the RAFT Process

propagating radical | RAFT agent | RAFT-adduct radical | polyRAFT agent | leaving group
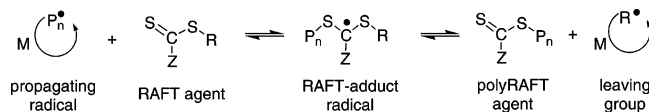
the corresponding non-RAFT system—has been observed.[1,12,13] This unusual rate retardation implies that there are elements of the RAFT mechanism (see below) that are not yet fully understood. Resolving these issues not only is important for the understanding of the RAFT process but has wider implications for radical chemistry in general.

The main point of controversy concerns the fate and stability of the RAFT-adduct radicals. To explain the rate retardation in systems such as cumyl dithiobenzoate (CDB)/styrene, some workers have suggested that the RAFT-adduct radical is a long-lived species,[12,14–24] whereas others have claimed that it is a short-lived radical that is consumed in bimolecular termination reactions.[13,25–28] In principle, a slow rate of reinitiation could also give rise to rate retardation effects. However, for the CDB/styrene system this can be safely ruled out on the basis of directly measured addition rate coefficients of the cumyl radical to styrene monomer.[29]

At the center of the controversy is the size of equilibrium constant, K, for the addition−fragmentation reaction.
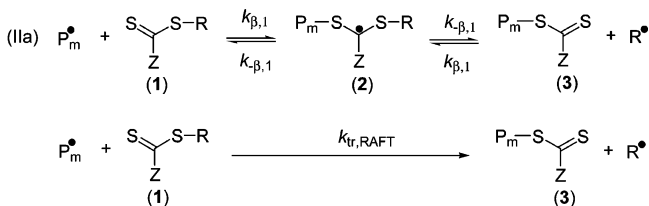
$$K = \frac{k_\beta}{k_{-\beta}} \quad (1)$$

where k_β and $k_{-\beta}$ are the rate coefficients of addition and fragmentation as defined in Scheme 2. An equilibrium constant can also be defined for the pre-equilibrium, where the initial thiocarbonylthio compound is converted to polymeric RAFT agent and where k_β and $k_{-\beta}$ are replaced by $k_{\beta,1}$ and $k_{-\beta,1}$. The existing dynamic rate and molecular weight data can be adequately described via the standard RAFT mechanism,[12,15,17]

(10) Krstina, J.; Moad, G.; Rizzardo, E.; Winzor, C. L.; Berge, C. T.; Fryd, M. *Macromolecules* **1995**, *28*, 5381−5385.
(11) See for example: Delduc, P.; Tailhan, C.; Zard, S. Z. *J. Chem. Soc., Chem. Commun.* **1988**, 308−310.
(12) Barner-Kowollik, C.; Quinn, J. F.; Morsley, D. R.; Davis, T. P. *J. Polym. Sci. Polym. Chem.* **2001**, *39*, 1353−1365.
(13) Monteiro, M. J.; de Brouwer, H. *Macromolecules* **2001**, *34*, 349−352.
(14) Barner-Kowollik, C.; Coote, M. L.; Davis, T. P.; Radom, L.; Vana, P. *J. Polym. Sci. Polym. Chem.* **2003**, *41*, 2828−2832.
(15) Barner-Kowollik, C.; Quinn, J. F.; Nguyen, T. L. U.; Heuts, J. P. A.; Davis, T. P. *Macromolecules* **2001**, *34*, 7849−7857.
(16) Vana, P.; Davis, T. P.; Barner-Kowollik, C. *Macromol. Theory Simul.* **2002**, *11*, 823−835.
(17) Perrier, S.; Barner-Kowollik, C.; Quinn, J. F.; Vana, P.; Davis, T. P. *Macromolecules* **2002**, *35*, 8300−8306.
(18) Zhang, M.; Ray, W. H. *Ind. Eng. Chem. Res.* **2001**, *40*, 4336−4352.
(19) Ah Toy, A.; Vana, P.; Davis, T. P.; Barner-Kowollik, C. *Macromolecules* **2004**, *37*, 744−751.
(20) Coote, M. L.; Radom, L. *J. Am. Chem. Soc.* **2003**, *125*, 1490−1491.
(21) Coote, M. L. *Macromolecules* **2004**, *37*, 5023−5031.
(22) Vana, P.; Quinn, J. F.; Davis, T. P.; Barner-Kowollik, C. *Aust. J. Chem.* **2002**, *55*, 425−431.
(23) Monteiro, M. J.; Bussels, R.; Beuermann, S.; Buback, M. *Aust. J. Chem.* **2002**, *55*, 433−437.
(24) Barner-Kowollik, C.; Vana, P.; Quinn, J. F.; Davis, T. P. *J. Polym. Sci. Polym. Chem.* **2002**, *40*, 1058−1063.
(25) Kwak, Y.; Goto, A.; Tsujii, Y.; Murata, Y.; Komatsu, K.; Fukuda, T. *Macromolecules* **2002**, *35*, 3026−3029.
(26) Kwak, Y.; Goto, A.; Fukuda, T. *Macromolecules* **2004**, *37*, 1219−1225.
(27) Kwak, Y.; Goto, A.; Komatsu, K.; Sugiura, Y.; Fukuda, T. *Macromolecules* **2004**, *37*, 4434−4440.
(28) Wang, A. R.; Zhu, S.; Kwak, Y.; Goto, A.; Fukuda, T.; Monteiro, M. S. *J. Polym. Sci. Polym. Chem.* **2003**, *41*, 2833−2839.
(29) Walbiner, M.; Wu, J. Q.; Fischer, H. *Helv. Chim. Acta* **1995**, *78*, 910−924.

Scheme 2. Reaction Set Used as the Basis for the Implementation of the RAFT Process in the PREDICI Program Package[32] *a*

I. INITIATION

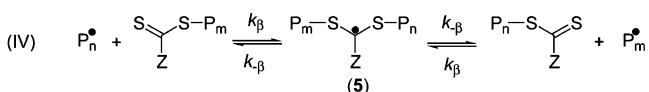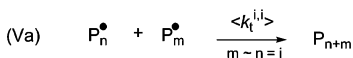(Ia)   Monomer $\xrightarrow{k_\gamma}$ $P_1^\bullet$

II. PRE-EQUILIBRIUM

(IIa) $P_m^\bullet + (1) \underset{k_{-\beta,1}}{\overset{k_{\beta,1}}{\rightleftharpoons}} (2) \underset{k_{\beta,1}}{\overset{k_{-\beta,1}}{\rightleftharpoons}} (3) + R^\bullet$

$P_m^\bullet + (1) \xrightarrow{k_{tr,RAFT}} (3) + R^\bullet$

III. PROPAGATION

(IIIa) $P_n^\bullet \xrightarrow[k_p]{Monomer} P_{n+1}^\bullet$ (IIIb) $R^\bullet \xrightarrow[k_i]{Monomer} P_1^\bullet$

IV. CORE EQUILIBRIUM

(IV) $P_n^\bullet + (5a) \underset{k_{-\beta}}{\overset{k_\beta}{\rightleftharpoons}} (5) \underset{k_\beta}{\overset{k_{-\beta}}{\rightleftharpoons}} (5b) + P_m^\bullet$

V. TERMINATION

(Va) $P_n^\bullet + P_m^\bullet \xrightarrow[m \sim n = i]{\langle k_t^{i,i}\rangle} P_{n+m}$

VI. CROSS TERMINATION

(5) $+ P_m^\bullet \xrightarrow[m \sim n = i]{\langle k_t^{cross\,i,i}\rangle}$ (6)
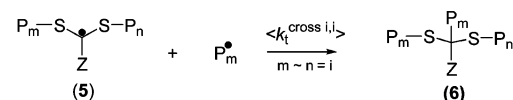
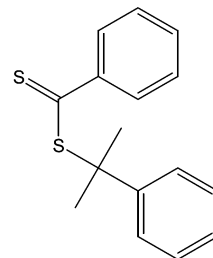*a* Not all displayed reactions were activated in each simulation and sensitivity analysis, depending on the type of analysis carried out. See text for details.

Scheme 3. Cumyl Dithiobenzoate (CDB)

Cumyl Dithiobenzoate (CDB)

provided the equilibrium constant is very high, i.e., $K > 10^6$ L mol^{-1}.[16] Since the rate of addition is known to be high (rate coefficients on the order of 10^6 L mol^{-1} s^{-1} have been reported for this system[12,25]), this implies that the RAFT-adduct radical in these systems is a relatively long-lived species. Such a notion is supported by high-level ab initio quantum mechanical calculations[20,21] as well as radical storage experiments.[24]

However, this high value for the equilibrium constant is inconsistent with the low radical concentrations that are observed via electron spin resonance (ESR) spectroscopy experiments.[25,26] In this regard, it should be noted that the existing ESR experiments have been performed under extremely forceful reaction conditions (such as ultrahigh initiator and RAFT agent concentrations), which bear little resemblance to controlled polymerization systems. Further ESR experiments under normal RAFT conditions would thus be desirable.

A low value for the equilibrium constant ($K < 100$ L mol^{-1})—implying fast fragmentation—is consistent with the ESR-determined intermediate radical concentrations and can be obtained if a cross-termination reaction involving propagating macroradicals and the RAFT-adduct radicals is added to the RAFT mechanism. However, although it has been demonstrated that coupling reactions involving the RAFT-adduct radical are certainly possible,[25,27,30] no evidence of star polymer formation has been found in polymerizing RAFT systems under normal reaction conditions, despite the use of ultrasensitive mass spectroscopic methods.[19] In this respect it should be noted that Tonge and co-workers[31] recently identified the products of coupling reactions involving the RAFT intermediate radical in polymerizing systems. However, they were careful to stress that these products were observed only in extremely low concentrations and under very forceful reaction conditions (i.e., very high initial RAFT agent concentrations) that bear little relation to actual polymerization systems. Although there is circumstantial evidence both for and against the cross-termination model, the ability of this model to describe the dynamic kinetic data of polymerizing RAFT systems has never been critically tested; the present study will provide such an assessment.

Identifying the stability and fate of the RAFT-adduct radical is important for designing RAFT agents and has wider implications, since thiocarbonylthio compounds are widely employed in organic synthesis as a convenient source of alkyl and acryl radicals.[11] In the present work we use a combination of careful kinetic measurements and high-level quantum mechanical calculations to provide a critical test of the cross-termination model. To provide this critical test, we examine the delayed onset of steady state in the cumyl dithiobenzoate (CDB)-mediated styrene polymerization at 30 °C. The alternative models provide significantly different predictions regarding this dynamic kinetic behavior. If slow fragmentation of the RAFT-adduct is the cause of rate retardation, the gradual conversion of propagating radicals to RAFT-adduct radicals delays the onset of steady state, and this should be evident in the shape of the conversion versus time data for the monomer. However, if the adduct is consumed in side reactions such as irreversible termination, then these should prevent the adduct from functioning as a radical sink, and steady state should be established almost immediately regardless of the magnitude of the equilibrium constant. The irreversible termination reactions should of course lead to retardation of the polymerization rate in the presence of the RAFT agent; however, such retardation should be evident throughout the course of the polymerization. These differences in the two alternative models are manifest in the qualitative shape of the time-dependent monomer conversion data.

In what follows we present measurements of the polymerization kinetics for cumyl dithiobenzoate (CDB, see Scheme 2) mediated styrene bulk polymerizations at 30 °C and use the

data to test the slow fragmentation and irreversible termination models. As part of this work, we estimate the equilibrium constant in the CDB/styrene system, using a novel methodology that is outlined below. We then compare this equilibrium constant with that obtained from ab initio molecular orbital calculations for the following small radical model of the pre-equilibrium in the CDB/styrene system at 30 °C.

$$(CH_3)_2C(Ph)^\bullet + S{=}C(Ph){-}S{-}CH_3 \rightarrow$$
$$(CH_3)_2C(Ph){-}S{-}C(Ph)^\bullet{-}S{-}CH_3 \quad (2)$$
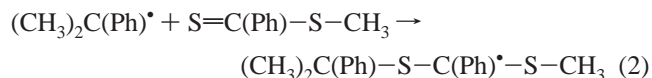
2. Methodology

In the present work, we introduce a new approach for estimating the equilibrium constant from time-dependent monomer conversion data *alone*. The monomer conversion versus time evolution was followed via on-line dilatometry with the polymerization process being initiated via γ-radiation. The choice of γ-radiation as initiation source was guided by the idea that the γ-radiation produces a constant radical flux over the entire reaction time, and this simplifies the kinetic analysis, since no recourse to the rates of the initiator decomposition is required. In the present study, the data were recorded at a CDB concentration of 5.5×10^{-3} mol L^{-1} and at a temperature of 30 °C.

In an earlier contribution, we demonstrated that, via a combination of time-dependent monomer conversion, polydispersity, and molecular weight data, solutions for k_β and $k_{-\beta}$ can be deduced via the PREDICI program package[32] based on an implementation of the RAFT mechanism originally suggested by the CSIRO group.[1] The PREDICI implementation of the RAFT process used in the current study is identical to the reaction steps displayed in Scheme 2. This scheme includes the standard RAFT mechanism with the addition of a possible irreversible cross-termination reaction between the intermediate macroRAFT radicals with propagating species. The full Scheme 2 is known as the cross-termination model; we also examined the standard RAFT mechanism (i.e., with cross-termination omitted). As part of this work we additionally tested a simplification of the pre-equilibrium (where it is replaced by a simple irreversible transfer reaction governed by $k_{tr,RAFT}$) as well as the influence of a chain length dependent cross-termination rate coefficient.

While the deduction of accurate values for both k_β and $k_{-\beta}$ requires both the polydispersity *and* conversion versus time data, the value of K can be deduced via the analysis of conversion data alone. Our analysis methodology yields several duplets of k_β and $k_{-\beta}$ that can adequately describe the experimental data. However, as will be demonstrated in this work, the ratio of each pair of k_β and $k_{-\beta}$ values always yields an identical value for the equilibrium constant. Because a range of duplets [k_β, $k_{-\beta}$] will allow for an adequate description of the conversion time data, our approach was to screen all possible combinations of k_β and $k_{-\beta}$ that will yield an adequate description of experimental data. This task was carried out via the *box search* function of the PREDICI program package in the intervals [$10^1 \leq k_\beta \leq 10^8$] and [$10^{-5} \leq k_{-\beta} \leq 10^6$] on a 9600 data point subdivision: A duplet [k_β, $k_{-\beta}$] is assumed, and using the kinetic data and

(30) Calitz, F. M.; McLeary, J. B.; McKenzie, J. M.; Tonge, M. P.; Klumperman, B.; Sanderson, R. D. *Macromolecules* **2003**, *36*, 9687−9690.
(31) Calitz, F. M.; Tonge M. P.; Sanderson R. D. *Macromolecules* **2003**, *36*, 5−8.
(32) Wulkow, M.; Busch, M.; Davis, T. P.; Barner-Kowollik, C. *J. Polym. Sci., Part A: Polym. Chem.* **2003**, *42*, 1441−1448.

parameters given in Table 1 (see below), the resulting conversion versus time functionality is computed for the predetermined CDB concentration (in this case 5.5×10^{-3} mol L^{-1}). The residual error between the computed and experimental monomer conversion versus time plot is calculated for each duplet and plotted in a contour plot. From this plot, the duplets of k_β and $k_{-\beta}$ that minimize the residual error are identified.

Prior to the screening analysis, the radical concentration generated by the γ source was determined. This is possible via a parameter estimation procedure for the given ratio of k_β and $k_{-\beta}$ (i.e., K) and the γ-induced radical concentration, c^γ, generated by the radiation. c^γ is independent of the value of K and can thus be assessed unambiguously. The value obtained was $c^\gamma = (6 \pm 1) \times 10^{-14}$ mol L^{-1}.

To implement the procedure, reliable values must be available for the rate coefficients of propagation, k_p,[33] initiation, k_i,[29] and termination, k_t (including its chain length dependency),[34-36] as well as for the density of styrene.[37] The chain length dependency of the termination rate coefficient, k_t, has recently been determined with high accuracy as a complete $\langle k_t^{i,i} \rangle$ versus i functionality in styrene bulk polymerization at 60 °C.[34,35] The entire functionality has been scaled according to an activation energy reported by Buback and co-workers for average termination rate coefficients, $\langle k_t \rangle$, in an identical system.[36] The complete $\langle k_t^{i,i} \rangle$ versus i data files for 30 °C can be found in the Supporting Information, as can the corresponding monomer conversion versus time evolution. The numbers employed in the analysis procedure are collated in Table 1. The value given in Table 1 for $k_{tr,RAFT}$ was calculated using an estimated activation energy of 26 kJ mol^{-1},[15] scaled according to the value for 60 °C given in ref 15. It should be noted that the magnitude of $k_{tr,RAFT}$ does not affect the size of the main-equilibrium constant when varied by several orders of magnitude.

3. Experimental Section

Materials. Styrene (Aldrich, 99%) was purified by passing over a column of basic alumina prior to use. Cumyl dithiobenzoate (CDB) was prepared using the method described by Oae et al.,[38] using *n*-hexane as the solvent. The purity of the RAFT agent was close to 99%, as verified by ^{1}H NMR and elemental analysis.[17]

Polymerizations. Solutions of styrene containing CDB (initial concentration close to 5.5×10^{-3} mol L^{-1}) or no CDB were thoroughly degassed under vacuum and transferred into a jacketed glass vessel. The vessel was connected to the dilatometer and an external water bath. The solutions were brought to reaction temperature (30 °C), and after a 30 min equilibration time the vessel was inserted into a ^{60}Co γ-source with a dose rate close to 0.2 kGy h^{-1}, for reaction times extending up

to 167 h. Monomer to polymer conversion was followed by dilatometry. The contraction factor was calculated from styrene and polystyrene densities available in the literature.[37]

Kinetic Modeling. All simulations have been carried out using the program package PREDICI, version 5.36.4a, on a Pentium IV (HT), 2.6 GHz IBM-compatible computer. A complete description of the implementation of the RAFT mechanism and the corresponding system of coupled ordinary differential equations can be found in ref 32.

Ab Initio Molecular Orbital Calculations. To complement the experimental data, the equilibrium constant for the pre-equilibrium in the styrene/CDB system at 30 °C was also estimated via ab initio molecular orbital calculations. These were performed on the model reaction shown in eq 2 and were carried out using the GAUSSIAN 03[39] software. Calculations were performed at a high level of theory, which was chosen on the basis of recent assessment studies for radical addition to double bonds.[40,41] Geometries of the reactants and products were optimized at the B3-LYP/6-31G(d) level of theory, and the vibrational frequencies were also calculated at this level. To ensure that the geometries were global, rather than merely local minimum energy structures, all alternative conformations of the reactants and products were first screened at the B3-LYP/6-31G(d) level of theory. Having obtained the globally optimized geometries, improved energies were then calculated at the RMP2/6-311+G(3df,2p) level of theory. The calculated geometries, frequencies, and energies were then used to calculate the equilibrium constant (and associated thermodynamic functions), using standard formulas, as outlined previously.[21,42] In calculating the partition functions, the low-frequency (<300 cm^{-1}) torsional modes were treated as one-dimensional hindered internal rotations. For each mode, full rotational potentials were obtained at the B3-LYP/6-31G(d) level of theory by performing a relaxed scan through the 360° in steps of 10°. These were then fitted with a Fourier series of up to 18 terms, and the corresponding energy levels were found numerically by solving the one-dimensional Schrödinger for a rigid rotor, using a Fortran program described previously.[43,44] Where the rotational potentials could be fitted with a simple cosine potential, the enthalpy and entropy associated with each mode were obtained from the Pitzer[45] tables. These two alternative approaches yield identical results for the special case of simple cosine potentials.

4. Results and Discussion

Model Discrimination. Figure 1 shows the evolution of the monomer conversion with reaction time for the styrene/CDB system at two initial CDB concentrations (i.e., $c_{CDB}^0 = 0$ and 5.5×10^{-3} mol L^{-1}) at 30 °C. Inspection of the figure shows that the reaction mixture where CDB is present displays a lower rate of polymerization and the shape of the conversion versus time graph is distinctly different from that observed in the conventional polymerization system. While the polymerization in the absence of CDB proceeds under steady-state conditions from the beginning, the CDB-mediated process shows a pronounced phase of non-steady-state behavior (i.e., a nonconstant rate of polymerization) up to reaction times of $t = 14$ h.

As explained above, the delayed onset of steady state is consistent with the slow fragmentation model, but not the irreversible cross-termination model. This qualitative failure of the irreversible termination model to describe the current experi-

(33) Buback, M.; Gilbert, R. G.; Hutchinson, R. A.; Klumperman, B.; Kuchta, F.-D.; Manders, B. G.; O'Driscoll, K. F.; Russell, G. T.; Schweer, J. *Macromol. Chem. Phys.* **1995**, *196*, 3267−3280.
(34) Feldermann, A.; Stenzel, M. H.; Davis, T. P.; Vana, P.; Barner-Kowollik, C. *Macromolecules* **2004**, *37*, 2404−2410.
(35) Vana, P.; Davis, T. P.; Barner-Kowollik, C. *Macromol. Rapid. Commun.* **2002**, *23*, 952−956.
(36) Buback, M.; Kuchta, F.-D. *Macromol. Chem. Phys.* **1997**, *198*, 1455−1480.
(37) Patnode, W.; Scheiber, W. J. *J. Am. Chem. Soc.* **1939**, *61*, 3449−3451.
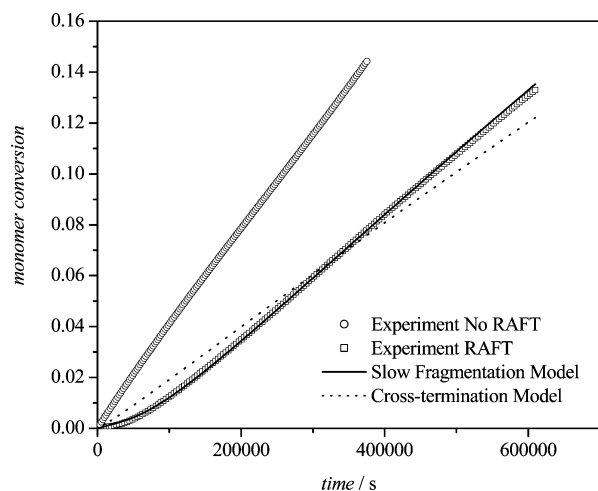(38) Oae S.; Yagihara T.; Okabe, T. *Tetrahedron* **1972**, *28*, 3203−3216.

Figure 1. Evolution of the monomer to polymer conversion with reaction time in the γ radiation-initiated bulk styrene free radical polymerization at 30 °C at two initial CDB concentrations, $c_{CDB}^0 = 0$ mol L^{-1} (circles) and $c_{CDB}^0 = 5.5 \times 10^{-3}$ mol L^{-1} (squares). The full line gives the best fit under the slow fragmentation model using the best-fit equilibrium constant of 1.06×10^7 L mol^{-1}. The dotted line corresponds to a "best fit" of the experimental data under the assumption that cross-termination involving the intermediate radicals (**5**) and propagating macroradicals is operative. The cross-termination rate coefficient was assumed to be chain length independent and half the size of the bimolecular termination rate coefficient (i.e., $\langle k_t^{cross} \rangle = 0.5 \langle k_t \rangle = 4.05 \times 10^7$ L mol^{-1} s^{-1})[25] A chain length dependent cross-termination rate coefficient (see text) does not significantly affect the simulation outcome.
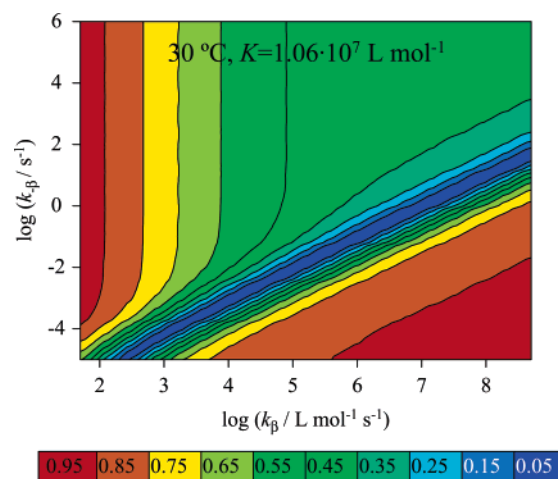

Figure 2. Residual error surfaces resulting from the sensitivity analysis of the experimental monomer conversion vs time data over a wide range of k_β ($10^1 \le k_\beta \le 10^8$) and $k_{-\beta}$ ($10^{-5} \le k_{-\beta} \le 10^6$) at 30 °C using the slow fragmentation model with a simplified pre-equilibrium. The straight valley of optimum experimental data representation corresponds to a uniform K value. The resulting value of K is 1.06×10^7 L mol^{-1}.

mental data is confirmed more quantitatively in the comparative fits of the slow fragmentation and irreversible termination models to the data. The best-fit predictions of the two alternative models are included in Figure 1, from which it can be seen that the slow fragmentation model can describe the data but not the irreversible cross-termination model. This kinetic analysis is now discussed in detail for each of the alternative models.

Model-Fitting: Slow Fragmentation Model. The slow fragmentation model was fitted to the time-dependent monomer conversion data via the methodology described above, so as to estimate the equilibrium constant. Initially, the pre-equilibrium was replaced with a simplified (and irreversible) transfer reaction governed by the rate coefficient $k_{tr,RAFT}$.[1,12] This simplification to the pre-equilibrium has no kinetic consequences, provided it is assumed that its corresponding rate coefficients (i.e., $k_{\beta,1}$ and $k_{-\beta,1}$) are similar to those of the main equilibrium. Such an approximation is certainly valid for the addition rate coefficient. The fragmentation rate coefficient of the pre-equilibrium is—if different from its counterpart in the main equilibrium—most certainly only larger (i.e., effecting a faster fragmentation), because a (tertiary) cumyl radical should be a slightly superior leaving group than a (secondary) polystyryl radical. Furthermore, were this not the case, then the propagating radical would fragment preferentially from the RAFT-adduct radical in the pre-equilibrium, and the initial RAFT agent would not be converted to poly-RAFT. Moreover, it has previously been demonstrated that the kinetic data measured using the polymeric RAFT agent in the styrene/CDB system (i.e., S=C(Ph)−PSTY) as the initial RAFT agent in styrene polymerization are virtually identical to that obtained with CDB itself under the same conditions.[22] This implies that the elimination of the pre-equilibrium (through the use of a poly-RAFT agent) does not eliminate the rate retardation.

The outcome of this analysis procedure can be adequately represented by depicting the residual error as a function of both k_β and $k_{-\beta}$ in a contour diagram (see Figure 2). Inspection of Figure 2 shows that a range of duplets [k_β, $k_{-\beta}$] can describe the experimental data equally well. It is thus impossible from recourse to monomer to polymer conversion data alone to deduce absolute numbers for the individual k_β and $k_{-\beta}$. However, the linear nature of optimum [k_β, $k_{-\beta}$] valley immediately shows that each ratio of k_β and $k_{-\beta}$ in this valley yields the same equilibrium constant, 1.06×10^7 L mol^{-1}. As seen above in Figure 1, using this estimated value of the equilibrium constant, the slow fragmentation model provides an excellent fit to the experimental data. The high value obtained for the equilibrium constant confirms that fragmentation of the RAFT-adduct radical is very slow (when compared with the reverse rate of addition), and it is this slow fragmentation that retards the rate of polymerization and delays the onset of steady state.

To confirm that the obtained equilibrium constant adequately describes the polymer formation process, we computed the full molecular weight distribution obtained after 600 000 s reaction time via the PREDICI program package. The resulting distribution was compared to the experimentally determined molecular weight distribution (via size exclusion chromatography) after the same reaction time. It is gratifying to note that both distributions are in excellent agreement. Both the experimental and computed full distributions (Figure S1), alongside the evolution of the number average molecular weight, M_n, and the polydispersity index, PDI, with reaction time (Figure S2) can be found in the Supporting Information. Also included in the Supporting Information are the complete evolutions of the major species (i.e., the initial RAFT agent, R group, propagating macroradicals, and intermediate macroRAFT radicals) with reaction time associated with the simulation depicted in Figure S2.

It is tempting to compare the equilibrium constant obtained at 30 °C with an earlier reported number for K in the same system at 60 °C ($K = 1.6 \times 10^7$ L mol^{-1}).[12] Both independently conducted approaches yield equilibrium constants in reasonable agreement with one another. The difference between the numbers is close to a factor of 1.5, and this may be the result

of both the temperature dependence of the equilibrium constant and the improved input parameters to the current analysis. In particular, the present analysis makes use of chain length dependent termination rate coefficient data, which was not available at the time when the analysis in ref 12 was carried out. Chain length dependent termination rate coefficient data can affect the analysis of free radical polymerization systems, especially in the short- and medium-length chain length regimes that are accessed via the RAFT process.

The above-described approach contains the simplification that the pre-equilibrium can be approximated with an irreversible transfer reaction governed by a single rate coefficient, i.e., $k_{tr,RAFT}$. Although it is plausible that this simplification is allowable (see above), it is mandatory to test whether the observed delayed onset of steady-state behavior can be caused by slow fragmentation in the pre-equilibrium alone. To assess this possibility, the full pre-equilibrium (as given by reaction step IIa in Scheme 2) was implemented in the PREDICI program package. For the polymerization process to proceed in a true living fashion, i.e., with the M_n versus conversion evolution passing through the origin, the initial addition rate coefficient, $k_{\beta,1}$, has to be sufficiently high. An insufficient rate of addition in the pre-equilibrium leads—irrespective of the magnitude of the fragmentation rate coefficient $k_{-\beta,1}$—to so-called hybrid behavior between living and conventional free radical polymerization.[15,16] Hybrid behavior manifests itself in an initial rapid increase of the molecular weight and a subsequent linear increase in M_n at a high molecular weight level. Since hybrid behavior is not a feature of CDB-mediated styrene polymerizations,[1,12] the value of $k_{\beta,1}$ was set to 4×10^6 L mol^{-1}.[25] For the main equilibrium, an identical value was assumed for k_β. We will demonstrate in detail below that high-level quantum mechanical calculations return an equilibrium constant of $K = 7.3 \times 10^6$ L mol^{-1} for the pre-equilibrium. In the kinetic analysis of the pre-equilibrium this number was employed, while—initially—the main equilibrium was assumed to have a low equilibrium constant of $K = 57$ L mol^{-1} ($k_\beta = 4 \times 10^6$ L mol^{-1} s^{-1} and $k_{-\beta} = 7 \times 10^4$ s^{-1}), values that were obtained under the cross-termination model.[26]

Inspection of Figure 3 clearly indicates that slow fragmentation in the pre-equilibrium alone cannot be responsible for the delayed onset of steady state, since the rate of polymerization with a pre-equilibrium constant of 7.3×10^6 L mol^{-1} is too rapid. The value obtained for the pre-equilibrium via molecular orbital calculations may have an uncertainty of up to 1 order of magnitude. For this reason, the conversion versus time profile for slow fragmentation in the pre-equilibrium was assessed for K values of 7.3×10^5 and 7.3×10^7 L mol^{-1}. It is evident from Figure 3 that even an extremely high equilibrium constant in the pre-equilibrium of close to 10^8 L mol^{-1} cannot reproduce the observed conversion versus time trace. If the quantum mechanical value for K is employed for the pre-equilibrium, a parameter estimation procedure (similar to the one described above) can be carried out to obtain a K value for the main equilibrium. The resulting main-equilibrium constant is close to a value of 8.9×10^6 L mol^{-1}, a fraction lower than the value obtained via the fitting procedure that assumed a simplified pre-equilibrium. Moreover, not unsurprisingly, the best-fit main-equilibrium constant is a fraction higher than the corresponding pre-equilibrium constant in the same analysis, confirming that
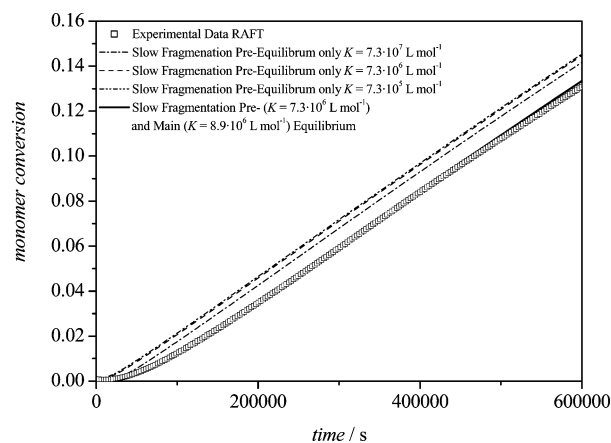

Figure 3. Sensitivity analysis of the influence of the pre-equilibrium on the monomer to polymer conversion vs time profile. The figure shows the effect of varying the magnitude of the equilibrium constant, K, in the pre-equilibrium (with a fixed value for $k_{\beta,1}$ of 4×10^6 L mol^{-1} s^{-1}) by 2 orders of magnitude from 7.3×10^7 to 7.3×10^5 L mol^{-1}. The full line represents the scenario when both the pre- and main-equilibrium constants have been set to a value of 7.3×10^6 and 8.9×10^6 L mol^{-1}, respectively. For details see text.

the pre-equilibrium constant provides a lower bound to the main-equilibrium constant. The above analysis of the pre-equilibrium has demonstrated that slow fragmentation in the pre-equilibrium *alone* is insufficient to explain the delayed onset of steady-state behavior in the CDB/styrene system. The main equilibrium has to display a high equilibrium constant as well.

Finally, we should note that in the above analysis we employed an identical rate coefficient, i.e., $k_{-\beta,1}$, for the fragmentation of the pre-equilibrium intermediate radical toward the release of the R-group and toward the release of the macro-radicals. In fact, the fragmentation rate coefficients for the loss of the R-group should actually be faster than for the loss of the macroradicals. If this were not the case, the macroradical would preferentially fragment from the RAFT-adduct radical, and the initial RAFT agent would not (or only very slowly) be converted to the polymeric-RAFT agent. Under such conditions, living behavior would not be observed. The rate coefficient for fragmentation of the polymeric radical from the initial RAFT-adduct radical ($P_n-SC^\bullet(Z)SR \rightarrow P_n^\bullet + S=C(Z)SR$) should be almost identical to that in the main equilibrium ($P_n-SC^\bullet(Z)SP_n \rightarrow P_n^\bullet + S=C(Z)SP_n$), since the radicals differ only in the nature of their remote substituent. We therefore carried out a kinetic analysis using the same value for the fragmentation of the polymeric radical in the pre-equilibria and main equilibria, but a different value for the fragmentation of the R-group. When the equilibrium constant associated with fragmentation of the R-group was fixed at the high value obtained from the ab initio calculations, we again found that the data could be fitted only if the equilibrium constant associated with fragmentation of the polymeric radical in the pre-equilibria and main equilibria was also high. In short, the delayed onset of steady-state cannot be attributed to slow fragmentation in the pre-equilibrium alone.

Model-Fitting: Irreversible Termination Model. To examine whether the introduction of an irreversible termination reaction for the intermediate macroRAFT radical with propagating macroradicals can describe the experimental data equally well, a further reaction pathway was introduced into the model, representing the irreversible termination step (see reaction step

VI in Scheme 2). For an in-depth coverage of the finer points of the implementation of a cross-termination reaction for the intermediate RAFT radical in PREDICI, the reader is referred to ref 32. For the following analysis, a simplified pre-equilibrium (see above) was implemented; however, the outcome of the reported simulations is identical when the pre-equilibrium is implemented in full. Fukuda and co-workers have recently suggested a potential value for the cross-termination rate coefficient, $\langle k_t^{cross} \rangle$, as being half the size of the conventional bimolecular termination rate coefficients.[25] Our current analysis employs an experimentally determined chain length dependent termination rate coefficient for conventional bimolecular termination. However, reported average termination rate coefficients for the same reaction conditions[36] have been used as the basis for calculating $\langle k_t^{cross} \rangle$; the effect of using a chain length dependent cross-termination rate coefficient will be addressed below. Thus, a value of 4.05×10^7 L mol^{-1} s^{-1} for $\langle k_t^{cross} \rangle$ at 30 °C was used.

The cross-termination model was fitted to the conversion time data so as to estimate the corresponding value of K that would yield an optimum description of the experimental data set. As noted above, the outcome of such an estimation attempt can to some extent be anticipated, since the presence of an intermediate termination pathway for species **5** will not allow for a sufficient radical sink to generate the non-steady-state conditions observed experimentally. In essence, the system will establish steady-state conditions almost immediately, regardless of the size of k_β and $k_{-\beta}$. The resulting poor fit of the model to the data is clearly evident in Figure 1. Not only is this model unable to fit the experimental data, it produces the wrong qualitative shape for the conversion versus time curve. Whereas the experimental data and predictions of the slow fragmentation model predict an initial non-steady-state period, the irreversible termination model predicts a steady (albeit retarded) rate from the beginning.

Owing to the poor fit of the model to the data, it is not sensible to estimate a value for the equilibrium constant under this model. Moreover, due to the poor fit of the model to the data, enormous differences can be obtained in the "best-fit" model predictions depending upon the method for weighting of residuals. In essence, it is either possible to describe the initial non-steady-state period with reasonable accuracy but suffer enormous errors in the conversions at longer times, or alternatively improve the description at longer times but at the expense of the initial period. A contour plot based on the latter alternative (and corresponding to the best-fit model predictions in Figure 1) is shown in Figure 4. Owing to the weighting of the residuals, it is not possible to make direct comparisons between the magnitude of the residual error under this model (Figure 4) and the slow fragmentation model (Figure 2), but the poor fit of the cross-termination model is clearly evident in Figure 1. Examining Figure 4, it is seen that the duplets that do provide the "best" (albeit poor) fit to the data under the irreversible termination model again fall on a straight line, yielding a "unique" (within that method of weighting the residuals) value of the equilibrium constant, 2×10^2 L mol^{-1}. As might be anticipated, this value is considerably smaller than that estimated under the slow fragmentation model, as the cross-termination reaction provides an alternative cause for rate retardation, and thus it is no longer necessary to attribute rate retardation to slow fragmentation of the RAFT-adduct radical.

In case the poor fit of the cross-termination model was due merely to the specific value chosen for the cross-termination coefficient, we also examined the fit of the model for other values. Not surprisingly, the fit of the model improved as the termination coefficient was decreased, down to a limit of 0, which of course corresponds to the slow fragmentation model. However, even at values of 10^3 L mol^{-1} s^{-1} (at which termination reaction would be barely observable for normal RAFT agent concentrations), the fit of the model remains noticeably poorer than that of the slow fragmentation model (see Figure 5). Once the cross-termination coefficient is dropped to a value of 10^2 L mol^{-1} s^{-1}, the fit of this model and the slow fragmentation model become virtually indistinguishable, and the K value becomes virtually identical to that obtained under the slow fragmentation model. However, at such a low rate coefficient, the cross-termination reaction is not significant under normal polymerization conditions and would be expected to occur (at low levels) only in the presence of excessive quantities of RAFT agent. Hence the experimental data are consistent with extremely low levels of cross-termination. However, at such levels, the reaction is not significant and cannot explain rate retardation under normal RAFT conditions.

It cannot be excluded a priori that a chain length dependence of the cross-termination rate coefficient, $\langle k_t^{cross} \rangle$, induces non-steady-state behavior at least to some extent. However, it can be anticipated that the effects are small, since the outcomes of the above analysis are not significantly changed if a chain length *independent* termination rate coefficient is used for the conventional termination between two propagating macroradicals. There are no reports of a functionality characterizing a potential chain length dependence of k_t^{cross} in the literature. However, should cross-termination reactions occur despite the evidence presented in this study, we anticipate that their chain length dependence is similar to that reported for the conventional bimolecular termination reaction and thus employed this functionality in our analysis.[34] The implementation of a chain length dependent cross-termination rate coefficient does not affect the shape of the corresponding curve, but rather slightly reduces the slope of the linear function. Thus, the result depicted in Figure 1 remains virtually unchanged, and it can be concluded that a chain length dependency of the cross-termination rate coefficient cannot be identified as the cause for the delayed onset of steady-state behavior in the CDB/styrene system.

In summary, it is clear that the cross-termination model cannot provide an adequate description of the experimental data for the CDB/styrene system.

Ab Initio Molecular Orbital Calculations. It is thus clear from the above model-fitting studies that the slow fragmentation model can be fitted to the current experimental data, but the leading alternative model (the irreversible cross-termination model) cannot. This provides strong experimental evidence that the irreversible cross-termination model—at least in its present form—is not applicable to the retarded styrene/CDB system. However, while this study also provides strong circumstantial evidence in favor of slow fragmentation, the possibility that there are additional complicating features in the reaction kinetics of RAFT polymerization cannot be ruled out. Under such circumstances, the estimated equilibrium constant obtained in a fit of the slow fragmentation model to the data would be merely a fit-parameter and would not reflect the true equilibrium constant
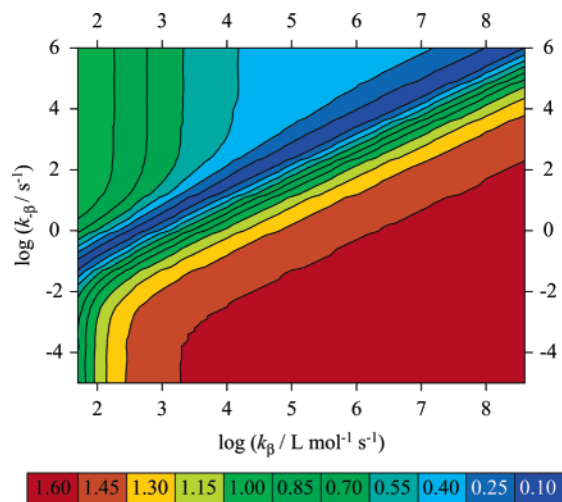
Figure 4. Residual error surfaces resulting from the sensitivity analysis of the experimental monomer conversion vs time data over a wide range of k_β ($10^1 \leq k_\beta \leq 10^8$) and $k_{-\beta}$ ($10^{-5} \leq k_{-\beta} \leq 10^6$) at 30 °C using the cross-termination model with a value for $\langle k_t^{cross}\rangle$ of 4.05×10^7 L mol^{-1} s^{-1}. The straight valley of optimum experimental data representation corresponds to a uniform K value. The resulting K value is 2×10^2 L mol^{-1}.

for the addition−fragmentation equilibrium. Hence, as a further test of the slow fragmentation model, we compared the measured equilibrium constant with that calculated directly, via ab initio molecular orbital calculations, so as to examine its likely physical validity.

The equilibrium constant (at 30 °C) was calculated for the pre-equilibrium in the model styrene/CDB system shown in eq 2. This model system matches the pre-equilibrium in the real RAFT system almost exactly, the only simplification being the use of a methyl group in the "nonparticipating position" of the RAFT agent (i.e., R′ in R′SC(Z)=S + •R). It has been demonstrated previously the R′-group does not significantly influence the reactivity of the RAFT agent.[1,46] The B3-LYP/6-31G(d) optimized geometries of the reactants and product in the model addition−fragmentation equilibrium are shown schematically in Figure 6, and the full geometries (in the form of GAUSSIAN archive entries) are included in the Supporting
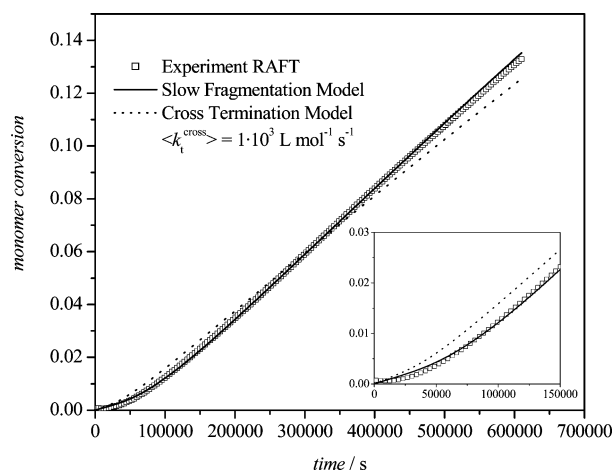
(39) Frisch, M. J.; Trucks, G. W.; Schlegel, H. B.; Scuseria, G. E.; Robb, M. A.; Cheeseman, J. R.; Montgomery, J. A., Jr.; Vreven, T.; Kudin, K. N.; Burant, J. C.; Millam, J. M.; Iyengar, S. S.; Tomasi, J.; Barone, V.; Mennucci, B.; Cossi, M.; Scalmani, G.; Rega, N.; Petersson, G. A.; Nakatsuji, H.; Hada, M.; Ehara, M.; Toyota, K.; Fukuda, R.; Hasegawa, J.; Ishida, M.; Nakajima, T.; Honda, Y.; Kitao, O.; Nakai, H.; Klene, M.; Li, X.; Knox, J. E.; Hratchian, H. P.; Cross, J. B.; Adamo, C.; Jaramillo, J.; Gomperts, R.; Stratmann, R. E.; Yazyev, O.; Austin, A. J.; Cammi, R.; Pomelli, C.; Ochterski, J. W.; Ayala, P. Y.; Morokuma, K.; Voth, G. A.; Salvador, P.; Dannenberg, J. J.; Zakrzewski, V. G.; Dapprich, S.; Daniels, A. D.; Strain, M. C.; Farkas, O.; Malick, D. K.; Rabuck, A. D.; Raghavachari, K.; Foresman, J. B.; Ortiz, J. V.; Cui, Q.; Baboul, A. G.; Clifford, S.; Cioslowski, J.; Stefanov, B. B.; Liu, G.; Liashenko, A.; Piskorz, P.; Komaromi, I.; Martin, R. L.; Fox, D. J.; Keith, T.; Al-Laham, M. A.; Peng, C. Y.; Nanayakkara, A.; Challacombe, M.; Gill, P. M. W.; Johnson, B.; Chen, W.; Wong, M. W.; Gonzalez, C.; Pople, J. A. *Gaussian 03, Revision B.03*; Gaussian, Inc.: Pittsburgh, PA, 2003.
(40) Coote, M. L.; Wood, G. P. F.; Radom, L. *J. Phys. Chem. A* **2002**, *106*, 12124−12138.
(41) Gómez-Balderas, R.; Coote, M. L.; Henry, D. J.; Radom, L. *J. Phys. Chem. A* **2004**, *108*, 2874−883.
(42) The formulas are provided in the Supporting Information of a recent publication: Coote, M. L.; Radom, L. *Macromolecules* **2004**, *37*, 590−596.
(43) Heuts, J. P. A.; Gilbert, R. G.; Radom, L. *J. Phys. Chem.* **1996**, *100*, 18997−19006.
(44) Nordholm, S.; Bacskay, G. B. *Chem. Phys. Lett.* **1976**, *42*, 253−258. Bacskay, G. B. Unpublished computer program, written in Fortran.
(45) Pitzer, K. S.; Gwinn, W. D. *J. Chem. Phys.* **1942**, *10*, 428−440. Li, J. C. M.; Pitzer, K. S. *J. Phys. Chem.* **1956**, *60*, 466−474.
(46) Chong, Y. K.; Krstina, J.; Le, T. P. T.; Moad, G.; Postma, A.; Rizzardo, E.; Thang, S. H. *Macromolecules* **2003**, *36*, 2256−2272.

Figure 5. Evolution of the monomer to polymer conversion with reaction time in the γ radiation-initiated bulk styrene free radical polymerization at 30 °C in the presence of 5.5×10^{-3} mol L^{-1} CDB (squares). The full line gives the best fit under the slow fragmentation model using the best-fit equilibrium constant of 1.06×10^7 L mol^{-1}. The dotted line corresponds to a "best fit" of the experimental data under the assumption that cross-termination involving the intermediate radicals (**5**) and propagating macroradicals is operative. The cross-termination rate coefficient was assumed to be chain length independent and equal to a value of 1×10^3 L mol^{-1}. A chain length dependent cross-termination rate coefficient (see text) does not significantly affect the simulation outcome.
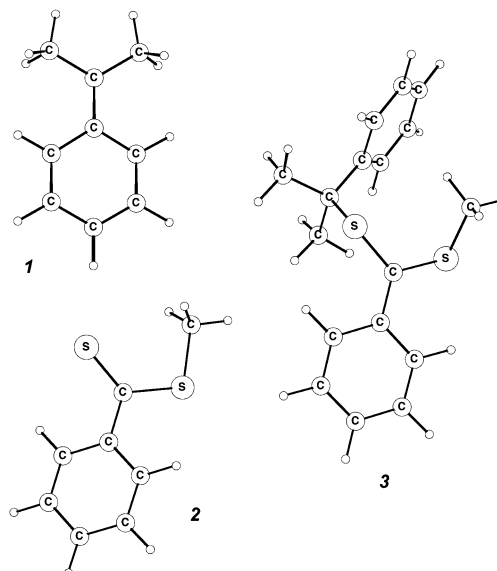

Figure 6. B3-LYP/6-31G(d) optimized geometries of the minimum energy conformations of the reactants and products in the model RAFT equilibrium.

Table 2. Equilibrium Constants, and Corresponding Thermodynamic Functions at 30 °C for the System Cumyl• + S=C(Ph)SCH$_3$ → Cumyl−SC•(Ph)SCH$_3$[a]

quantity	value (at 30 °C)
ΔS/J mol^{-1} K^{-1}	−153.1
ΔH/kJ mol^{-1}	−78.1
ΔG/kJ mol^{-1}	−31.7
K(theory)/L mol^{-1}	7.3×10^6
K(experiment)/L mol^{-1}	1.06×10^7

[a] Calculations at the RMP2/6-311+G(3df,2p)//B3-LYP/6-31G(d) level of theory and based on the hindered rotor model (see text).

Information. The equilibrium constant for this system and its enthalpic and entropic components are shown in Table 2. The corresponding experimental value of the equilibrium constant,

as estimated from the fit of the slow fragmentation model to the current experimental data, is also included in Table 2 for purposes of comparison.

Examining Table 2, we note that the agreement between the calculated and experimental values of the equilibrium constant at this temperature is excellent, which in turn indicates that the equilibrium constant estimated by fitting the slow fragmentation model to the experimental data is likely to be physically realistic. Although the calculated equilibrium constant is approximately 30% lower than the experimental value, this difference can be largely explained by the influence of the solvent in the polymerization system. In the present work, the theoretical calculations are based on the statistical thermodynamics of an ideal gas, whereas the polymerization takes place in the solution phase. As discussed previously,[21] for bimolecular association reactions (i.e., A + B → C), the entropy of reaction is generally lower in the gas phase, compared with the solution phase, and the solution-phase equilibrium constants are expected to exceed the (calculated) gas-phase values by approximately 1 order of magnitude.[47] As discussed above, in all other respects the calculated values are expected to be directly indicative of the pre-equilibrium in the polymeric system, given that the leaving group (cumyl) and Z-substituent (phenyl) on the RAFT agent are matched exactly, and the R′-group (which is simplified in the calculations) is not expected to affect the reactivity of the RAFT agent. The calculations thus indicate that the pre-equilibrium constant is high, and thus, given that the accepted values for the addition rate coefficients are fast (ca. 10^6 L mol^{-1} s^{-1}),[12,25] the calculations confirm that the fragmentation of the initial RAFT-adduct radical is slow.

The calculated equilibrium constant also supports the notion that fragmentation in the main equilibrium is also slow, since, as discussed above, the pre-equilibrium constant should, if anything, provide a *lower* bound to the main-equilibrium constant. In other words, we argue that the *tertiary* cumyl radical, being both more stable and more hindered than the *secondary* poly-styryl radical, should be a more effective leaving group. If this were not the case, the propagating radical would preferentially fragment from the RAFT-adduct radical in the early stages of the reaction, and the initial RAFT agent would not be converted to the polymeric RAFT agent. (If the fragmentation rate constants were close enough, slow conversion to poly-RAFT might occur, but under such circumstances the control would be poor, which is not the case in the present system.) Previously, calculations using a simpler model of the pre/main equilibrium in this system (i.e., using a benzyl rather than cumyl leaving group) were also used to support the notion of slow fragmentation,[21] and the present study (in which more accurate calculations have been performed on a larger chemical

model) confirms these earlier findings. In short, the ab initio calculations indicate that the RAFT-adduct radical is a relatively stable radical, and the calculated equilibrium constants are in accord with the experimental values that are estimated under the assumptions of the slow fragmentation model.

5. Conclusions

In the present work we have demonstrated that the cross-termination model comprehensively fails to describe the kinetic data for the CDB/styrene system. In particular, it fails to capture the delayed onset of steady state. At the same time, we have shown that the slow fragmentation model can provide an adequate fit to the data, provided the equilibrium constant is high in the main equilibrium. Such a high equilibrium constant is supported by high-level quantum chemical calculations and implies that the RAFT-adduct radicals are long-lived species in this system. The present mechanistic interpretation of the RAFT process is able to reconcile all available experimental and quantum chemical data, except for the low radical concentrations observed in ESR experiments. However, as indicated in the Introduction, these experiments have been performed under extreme conditions (e.g., ultrahigh initial RAFT agent and initiator concentrations > 0.2 mol L^{-1} and usage of a macroRAFT agent), which bear little resemblance to living free radical polymerization systems. The slow fragmentation of the RAFT-adduct radical leads to a buildup of the intermediate radicals, which in turn increases the probability that irreversible termination pathways can become operative. Thus, it comes as no surprise that, at extremely high RAFT agent concentrations, some irreversible termination products are indeed observed. However, it is important to note that the defining kinetic characteristic of the polymerizing systems, and thus the underlying cause for rate retardation, is the slow fragmentation of the intermediate macroRAFT radicals.

Supporting Information Available: The conversion versus time and the chain length dependent k_t data, the B3-LYP/6-31G(d) optimized geometries (in the form of GAUSSIAN archive entries) for the species used in calculating the equilibrium constants, the calculated and experimental molecular weight data, and the associated major species concentration evolutions are available free of charge via the Internet at http://pubs.acs.org.

JA046292B

(47) Whereas in the gas phase the reactants have translational and rotational degrees of freedom, in the solution phase these modes are effectively "lost" in collisions with the solvent. In their place, the solution-phase system has additional modes (that can loosely be thought of as vibrations) reflecting the interaction of the solute with the solvent, but these modes generally contribute less to the total entropy of the system. Since, in a bimolecular association reaction, 3 translational and 3 rotational modes are "lost" upon reaction, the entropy that is lost in a gas-phase reaction is thus larger than that which is lost in the corresponding solution-phase reaction. Hence, the equilibrium constant is higher in the latter case. While it is difficult to estimate this (entropically based) gas-phase/solution-phase difference exactly, a reasonable estimate can be made by comparing experimental gas-phase and solution-phase rate coefficients for radical addition reactions, with the latter generally exceeding the former by approximately 1 order of magnitude [see for example: Fischer, H.; Radom, L. *Angew. Chem., Int. Ed.* **2001**, *40*, 1340−1371].